Remote Sensing Applications: Society and Environment 33 (2024) 101144

Contents lists available at ScienceDirect

Remote Sensing Applications: Society and Environment

journal homepage: www.elsevier.com/locate/rsase

An analysis of the effects of changes in land use and land cover on runoff in the Luvuvhu catchment, South Africa

Mpho Oscar Mabuda[a], Cletah Shoko[b], Timothy Dube[a,*], Dominic Mazvimavi[a]

[a] Institute for Water Studies, University of the Western Cape, Robert Sobukwe Road, Bellville, 7535, South Africa
[b] Department of Geography, School of Geography, Archaeology and Environmental Studies, University of Witwatersrand, Johannesburg, South Africa

ARTICLE INFO

Keywords:
Hydrological modelling
Machine learning
Remote sensing
Surface runoff

ABSTRACT

The aim of this study was to map and assess the impacts of land use and land cover (LULC) changes on runoff in the Luvuvhu catchment in Limpopo, South Africa. To achieve this, the study determined past spatial trends of LULC change, using Landsat images from 1990 to 2020 and Support Vector Machine (SVM). The study also predicted future LULC in 2025 and 2030 using artificial neural networks-cellular automata (ANN-CA) simulation model, as well as established the response of runoff to LULC changes, using Soil and Water Assessment Tool (SWAT) model. The results revealed significant LULC changes in the Luvuvhu catchment during the study period. Bare land had the largest increase of 15.2% whereas natural vegetation had the largest decrease of 18.9%. The LULC classification results showed high overall accuracies ranging from 93% to 98% and Kappa coefficients above 0.9. The predicted LULC for 2025 show that bare land will have the largest increase of 168 km^2 whereas natural vegetation may lose the largest area of 356 km^2 in 2025. The same trends observed in 2025 are expected to continue to the year 2030. Results further indicated that, on average, overall surface runoff increased by 7.3% from 169.14 mm to 181.49 mm between 1990 and 2020. The results showed that the surface runoff of the Luvuvhu catchment was altered due to the significant LULC changes in bare land and natural vegetation with 15.2% increase and 18.9% decrease, respectively. Therefore, these changes contributed significantly to the runoff response of the Luvuvhu catchment. Owing to the anticipated ongoing LULC alterations, the likelihood of increased surface runoff persists, posing potential catchment management challenges, including flooding and erosion of riverbanks or stream channels. Hence, prioritizing the development of effective catchment management strategies is crucial, serving as a pivotal measure to mitigate the impacts of LULC changes. This study provides baseline information on the impacts of LULC changes on surface runoff within the Luvuvhu catchment in Limpopo, South Africa.

1. Introduction

Land use and land cover (LULC) change is a key factor that affects the Earth's system processes (Lambin et al., 2001). The evolving human population, climate change and natural occurrences drive successive LULC changes. LULC changes occur to primarily support the increasing human population, with great loss of natural vegetation cover due to settlement establishment (Getahun and Haj, 2015; Yadav, 2019). Furthermore, the effects of climate change affect crop production and leads to loss of natural forest cover (Thapa, 2021). Land cover reflects ecological and hydrological processes within a catchment. Therefore, changes in a catchment will signifi-

* Corresponding author.
E-mail address: tidube@uwc.ac.za (T. Dube).

https://doi.org/10.1016/j.rsase.2024.101144
Received 25 August 2023; Received in revised form 16 January 2024; Accepted 17 January 2024
Available online 18 January 2024

cantly affect the hydrological and terrestrial ecosystems of that area by changing the physical structure of the landscape and water fluxes (Turner et al., 2003; Maviza and Ahmed, 2020). Furthermore, LULC changes affect the water cycle by changing the magnitude and timing of runoff due to changes of evapotranspiration, infiltration, and the rate of runoff generation (Sterling et al., 2012; Guo et al., 2020; Anand et al., 2018). Similarly, Peng & Wang (2012) stated that LULC changes and rainfall patterns affect the intensity and frequency of surface runoff. Factors such as rainfall intensity, slope steepness and change of energy influence runoff generation (Gessesse et al., 2014; Ozdemir and Elbaşı, 2014). The increase in surface runoff often leads to flooding and increased annual discharge (Ntanganedzeni and Nobert, 2020). Therefore, understanding the relationship that exists between LULC changes, hydrologic processes, and their response at catchment scale remains imperative for better land use planning and management of catchments is crucial.

Remote sensing has proven to be an invaluable approach for LULC change monitoring over time across the globe at various scales (e.g., Abd El-Kawy et al., 2011). In addition, studies such as (Abijith and Saravanan 2022; Rahman et al., 2017; Singh et al., 2022; Bagaria et al., 2021) have also successfully predicted future LULC changes, using remote sensing, environmental factors, and prediction models. Similarly, within the hydrological field, the potential of remote sensing has been widely identified (Jewitt et al., 2004; Griscom et al., 2009; Warburton et al., 2012; Zhang et al., 2014; Mathivha et al., 2016). Remotely sensed data provide the spatial and temporal information needed for hydrological modelling. Different hydrological models have been developed and applied to understand hydrological processes (Lin et al., 2015; Devia et al., 2014, 2015). For example, Shoko et al. (2015), modelled evapotranspiration, using MODIS and Landsat remote sensing datasets and the Surface Energy Balance SEBS model for the uMngeni Catchment in South Africa.

Previous studies that assessed LULC change affected the hydrological response in the Luvuvhu catchment have reported fairly comparable results although they used different hydrological modelling approaches. These studies show an increase in peak discharges in the Luvuvhu catchment due to deforestation (Warburton et al., 2012; Mathivha et al., 2016; Thavhana et al., 2018). While previous studies have evaluated the impacts of LULC changes, it is crucial to investigate potential future impacts to bolster our understanding. Therefore, evaluating the impacts of LULC change using a physical based hydrological modelling approach for different LULC periods is still imperative. Further research in this area not only contributes to enhancing our knowledge but also supports land restoration initiatives. This study aims to analyze both historical and projected spatial trends of LULC changes, as well as to elucidate the effects of these changes on runoff within the Luvuvhu catchment, South Africa. Employing a physically based hydrological modeling approach to evaluate the impacts of LULC changes across different time periods in the Luvuvhu catchment remains essential. Consequently, this study integrates the use of remotely sensed data and a physical-conceptual semi-distributed modelling approach to comprehensively examine the response of runoff to LULC changes in the Luvuvhu catchment, South Africa.

2. Materials and methods

2.1. Study area

The Luvuvhu catchment is situated in the Limpopo Province, South Africa (Fig. 1). The Luvuvhu catchment is located between latitudes 22°17′57"S and 23°17′31"S and longitudes 29°49′16"E and 31°23′02"E and covers an area of approximately 5941 km^2. This catchment is situated in the Luvuvhu/Letaba Water Management Area. The catchment mainly consists of rural settlements, commercial agriculture, and the Kruger National Park, with three major urban centres, which are Malamulele, and Thohoyandou, Louis Trichardt (Hope et al., 2004; Odiyo et al., 2012). The upper region of Luvuvhu catchment consists of narrow, steep small rivers that drain into the Luvuvhu River. Furthermore, the Luvuvhu catchment has three major dams namely, Vondo Dam, Albasini Dam and Nandoni Dam (Hope et al., 2004). The climate in the Luvuvhu catchment varies from humid sub-tropical to semi-arid climate. The western part of the Luvuvhu catchment is characterised by a dry, hot semi-arid climate, while the eastern part is more humid with subtropical temperatures (Hope et al., 2004). High temperatures are experienced between October to February and low temperatures between May to July. The mean annual temperature ranges from 18 °C in the southwest region to 24 °C in the north-eastern plains of the catchment (Odiyo et al., 2012). Rainfall is seasonal and occurs mainly during summer months (October to April). The catchment has mean annual precipitation of 608 mm/year, rising from 300 mm/year in the dry lower areas of the catchment to 1870 mm/year in the mountainous upper areas of the catchment (Odiyo et al., 2012).

2.2. Remote sensing data collection and preprocessing

Landsat data (Landsat 5 TM and Landsat 8 OLI) at 30m spatial resolution were used to determine LULC change in the study area. The data were chosen based on freely accessibility, and archive data for change detection. The images were acquired from the United States Geological Survey (USGS) website (https://earthexplorer.usgs.gov/). Table 1 highlights the characteristics of selected Landsat series images.

Table 2 further illustrates the image acquisition dates which were selected based on data availability and cloud cover. All images were acquired between June and October, which is a dry season in the area.

The acquired Landsat images were geo-referenced to the Universal Transverse Mercator (UTM) zone 36S with World Geodetic System (WGS) 1984 projection in the ArcGIS environment. Landsat bands for each period were stacked in layers to create a multiband image and then subset to cover the study area. Image preprocessing was achieved using FLAASH tool in ENVI.

2.3. Reference data collection

The red, green blue bands, from both sensors were combined to create a true colour composite to gather representative samples of the six LULC types. The classes considered in this study are presented in Table 3. Depending on the availability of Google Earth Pro

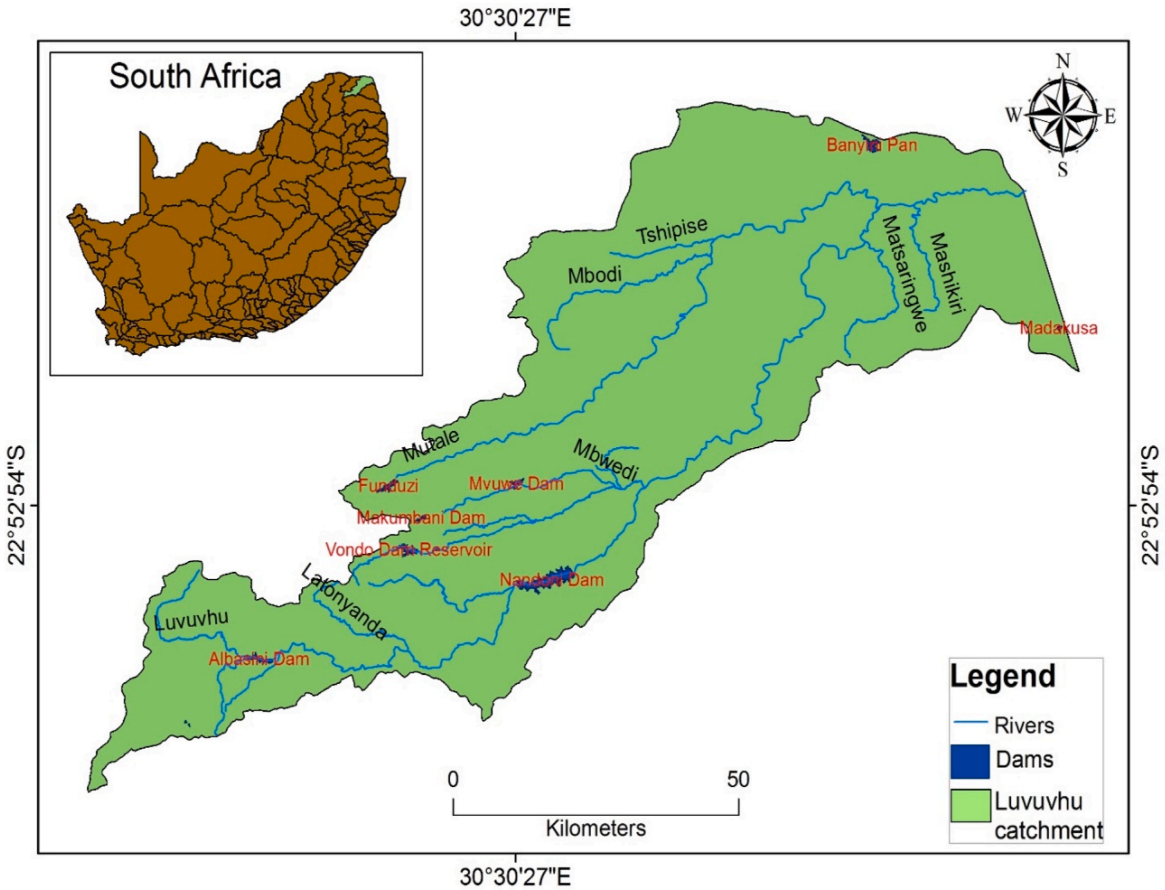

Fig. 1. Location of the Luvuvhu catchment in Limpopo, South Africa.

Table 1
Characteristics of Landsat imageries used in this study.

Landsat Sensor	Band Name	Bandwidth (μm)
Landsat 5 TM	Band 1 (Blue)	0.45-0.52
	Band 2 (Green)	0.52-0.60
	Band 3 (Red)	0.63-0.69
	Band 4 (Near infrared)	0.76-0.90
	Band 5 (Shortwave Infrared)	1.55-1.75
	Band 7 (Shortwave Infrared)	2.08-2.35
Landsat 8 OLI	Band 2 (Blue)	0.43-0.45
	Band 3 (Green)	0.53-0.59
	Band 4 (Red)	0.64-0.67
	Band 5 (Near Infrared)	0.85-0.88
	Band 6 (Shortwave Infrared)	1.57-1.65
	Band 7 (Shortwave Infrared)	2.11-2.29

images acquired during or close to the acquisition dates of the Landsat images, Google Earth Pro was also used as an additional tool for gathering LULC samples.

Representative samples of LULC classes were extracted as regions of interest (ROIs), which were then examined for class separability using Transformed Divergence (TD) and Jeffries-Matusita Distance (JMD). Separability measures between different LULC classes are necessary for the evaluation of quality of the samples representative of the LULC classes in order to avoid misclassification (Powell et al., 2004). The TD and JMD separability measures of classes pairs indicate how well the classes separate and are reported as values in the range of 0–2; where 2 indicates perfect separation of the two classes and 0 shows complete overlap between the spectral signatures of two classes (Richards and Jia, 2005), while ≥1.5 indicates acceptable separability between classes (Latty and Hoffer, 1980). In general, values greater than 1.9 between two classes indicate excellent separability (Richards and Jia, 2005).

Table 2
Details of Landsat datasets used in this study.

Scene ID	Acquisition Date	Path/Row
LT05_L2SP_169076_19901006_20200915_02_T1	1990/10/06	169/076
LT05_L2SP_169076_19950801_20200912_02_T1	1995/08/01	169/076
LT05_L2SP_169075_19950801_20200912_02_T1	1995/08/01	169/075
LT05_L2SP_169076_20000830_20200906_02_T1	2000/08/30	169/076
LT05_L2SP_169076_20050913_20200901_02_T1	2005/09/13	169/076
LT05_L2SP_169076_20100506_20200824_02_T2	2010/05/06	169/076
LT05_L2SP_169075_20100506_20200825_02_T2	2010/08/06	169/075
LC08_L2SP_169076_20150808_20200908_02_T1	2015/08/08	169/076
LC08_L2SP_169076_20200504_20210508_02_T1	2020/05/04	169/076

Table 3
Major LULC characterizing the study area.

LULC type	Description
Waterbody	Natural and man-made surface water bodies (rivers, streams, dams, etc.)
Built-up	Settlements, public utilities, industrial and commercial complexes, roads,
Bare Land	Unoccupied and virgin land either characterized by soils and/or rocks
Plantation	These were mainly planted commercial trees
Natural vegetation	Forest, trees, shrubs, bushes, and grass of natural origin (sparse and dense), aquatic plants
Agricultural Land	This includes cumulative land occupied by different crops

2.4. Ancillary data collection and preprocessing

A Digital Elevation Model (DEM) with 30m spatial resolution was acquired from the Shuttle Radar Topography Mission (SRTM). The DEM was used to derive elevation, slope and stream network for modelling with the SWAT model. Conventional data of landform (in a vector format) was also acquired from Soil and Terrain Database for South Africa. A soil map is also a prerequisite input for running the SWAT model and was obtained from the Food and Agriculture Organisation of the United Nation. The meteorological data used during simulation were obtained from the Agricultural Research Council (ARC) for 6 stations located in the Luvuvhu catchment. The climate data includes precipitation relative humidity, wind speed, minimum and maximum temperatures from 1990 to 2020. The weather stations used in this study were selected based on data availability and their distribution within the Luvuvhu catchment.

3. Image classification

Support Vector Machine (SVM) algorithm was used for classification. The algorithm is a non-parametric machine-learning algorithm (Richards and Jia, 2005) capable of overcoming the inherent drawback of the parametric classification algorithm such as Maximum Likelihood (ML) and other non-parametric algorithm such as Neural Network (NN) machine learning algorithm (Manoj et al., 2013). In addition, SVM algorithm appears to be incredibly dependable when dealing with heterogeneous classes when the number of training samples is small (Lothar et al., 1999). The superior performance of the SVM in LULC mapping was demonstrated in the study of Muavhi (2020) which was conducted in the same region. In different studies, reported that SVM produced relatively high accuracies compared to ML, NN and Decision Tree techniques, whereas Manoj et al. (2013) highlighted better overall accuracy from SVM compared to ML.

3.1. Accuracy assessment and change detection

Accuracy assessment for the classified images was done using overall accuracy, Kappa coefficient, user's and Producer's accuracies. These are common accuracy techniques using in remote sensing. The accuracy of LULC maps is evaluated empirically by checking the number of sample points assigned to each LULC class compared to the reference data or ground truth data, which is also referred to as validation data (Richards and Jia, 2005). Based on this approach, the percentage of pixels from each class in the image labelled correctly by the classification algorithm can be estimated together with the percentage of pixels from each class incorrectly labelled into every other class (Richards and Jia, 2005). A simple post-classification comparison method was implemented to detect LULC changes over the period of 30 years from 1990 to 2020. This approach was considered because it quantifies rate and magnitude of change. The, from-to change information is achieved by the comparison of the classified LULC maps on a pixel-by-pixel basis (Ban and Yousif, 2016; Alawamy et al., 2020).

3.2. LULC predictions modelling

The Cellular Automata (CA) model was implemented to simulate the future LULC dynamics using the Modules of Land Use Change Evaluation (MOLUSCE) plugin from QGIS 2.18 software. CA model enables clear insights into global and local patterns of LULC changes by relating the new state to its previous state (Santé et al., 2010). The CA model can predict and model the spatial distribution of the LULC pattern including its dynamics since it can add spatial properties of LULC (Santé et al., 2010), by utilizing the condition of nearby cells for its transition principles (Ghosh et al., 2017). On the other hand, MOLUSCE analyses, models, and simulates LULC changes by incorporating well-known algorithms which include CA, logistic regression (LR), weights of evidence (WoE), artificial neural networks (ANN) and multi-criteria evaluation (MCE) (MOLUSCE, 2018). MOLUSCE user interface provides simplistic interface with specific functions and modules. The CA takes input factors (LULC and spatial variables) and models (ANN, LR, WoE or MCM), meanwhile the simulator takes the probabilities of transition from the transition matrix, and then initiates a model and offers it with input factors (Jogun et al., 2019; Yatoo et al., 2020). For every class, potential transitions are estimated, and the simulator establishes a raster of the most probable transitions. In this regard, each transition belonging to most probable transitions, the simulator searches a fixed number of pixels with the highest certainty and then changes the class of the pixels (Yatoo et al., 2020). For this study, the generated LULC maps for 2010 and 2015 were used as initial (first) and final (second) LULC maps and elevation, slope, landform, and distance to stream were considered independent spatial variables. MOLUSCE-based Multi-Layer Perception (MLP), which is the most utilized form of ANN was used for transitional modelling of LULC change. Researchers (MOLUSCE 2018; Hakim et al., 2019; Yatoo et al., 2020; Thanekar and Krishna, 2021) have applied ANN algorithm owing to its optimal accuracy compared to other algorithms.

3.3. Validation of predicted LULC

In MOLUSCE plugin, validation is conducted between the reference map (actual third year LULC) and simulated map (third year LULC prediction) by calculating the overall accuracy (% of correctness) and Kappa statistics (i.e., overall Kappa, histogram Kappa and location Kappa). When the overall accuracy and Kappa statistics are according to the assessment standard, the CA simulation stage is then used to predict or model the future LULC trends (Equation (1)). The year of prediction depends on the number of iterations multiplied by the second year minus the first year (Hakim et al., 2019). In this study, the iteration values of 2 and 3 were used for the projection of 2025 and 2030, respectively.

$$S(t, t+1) = f(S(t), N) \tag{1}$$

Where *S (t + 1)* is the system status at the time of *(t, t + 1)*; functioned by the state probability of any time (N).

3.4. Modelling the impact of LULC changes on run-off

The SWAT model was used to predict the impacts of LULC on run-off. SWAT is a hybrid model that operates on the physical processes within the catchment but employs conceptual and empirical algorithms to compute hydrological characteristics (J. G. Arnold et al., 2012; Sidle, 2021). More details on how the SWAT model works are detailed by Arnold et al. (2012) and Affessa et al. (2022). The SWAT model was run as an extension (QSWAT) on QGIS 3.16.8. The spatial data used during surface runoff simulation were digital elevation model obtained from USGS, LULC maps, and soil data from the Food and Agriculture Organisation (FAO) of the United Nation with a spatial scale of 1: 5 000 000. The meteorological data used during simulation were obtained from the Agricultural Research Council (ARC) for 6 stations located in Luvuvhu catchment, these include daily rainfall, temperature, and relative humidity. Hydrological simulation analysis for the assessment of surface runoff response to LULC changes was determined by the SCS Curve Number approach. The simulation of the surface runoff was conducted for two land use periods, 1990 and 2020. The climatic data, soil map and topography used during simulation of the two land use scenarios was kept constant, while the LULC period map was changed. The calibration and validation of the model were both conducted using SUFI-2 algorithm in SWAT-CUP. This study made use of the split-sampling method, dividing the observed data into calibration and validation data to ensure data independence. Components of the water balance such as surface runoff, evapotranspiration and water yield were considered in the assessment of hydrological response to LULC changes after calibration of the model.

3.5. Model performance evaluation

Three criteria were used to evaluate SWAT model performance. The model evaluation was based on statistical criteria, which include the Nash-Sutcliffe efficiency (NSE), the coefficient of determination (R^2), and percent bias (PBIAS). Each performance parameter pertains to a specific purpose during the comparison of observed and simulated flows. NSE ranges from −0 to 1, the closer the NSE values is to 1, the higher the accuracy of the model. R^2 represents the strength of linear correlation that exists between the observed and simulated data and ranges from 0 to 1. R^2 values greater than 0.5 show less error variance and are therefore acceptable measures. PBAIS measures the tendency of the resulting simulated data to be higher or lower than the observed data (Abbas et al., 2016). A positive PBIAS value indicates model underestimation, while a negative PBIAS value shows model overestimation (Moriasi et al., 2007a, b). Detailed summary of the data analysis methodology is provided on the flowchart (Fig. 2).

4. Results

4.1. Accuracy assessment of image classification

Table 4 illustrates the accuracy assessment results associated with the classification using Landsat and SVM. High overall accuracies were produced, ranging from 93% to 98% and Kappa coefficients above 0.9. The year 2020 attained the highest Kappa coefficient and overall accuracy, in contrast these main accuracy measures were the lowest for 1995 classification image. LULC classes attained an estimated producer's accuracy (PA) and user's accuracy (UA) of ≥70%, and commission error (CE) and omission error (OE) of <30% for all classified images. The confusion matrix reported a PA of <80% for built-up areas in 1990, 1995, 2000 and 2010. These were the years in which built-up areas achieved the lowest PA. However, in the later years of the study period i.e., 2015 and 2020, built-up reached a PA of 90%. Waterbody, natural vegetation, and bare land attained PA beyond 90% for the entire study pe-

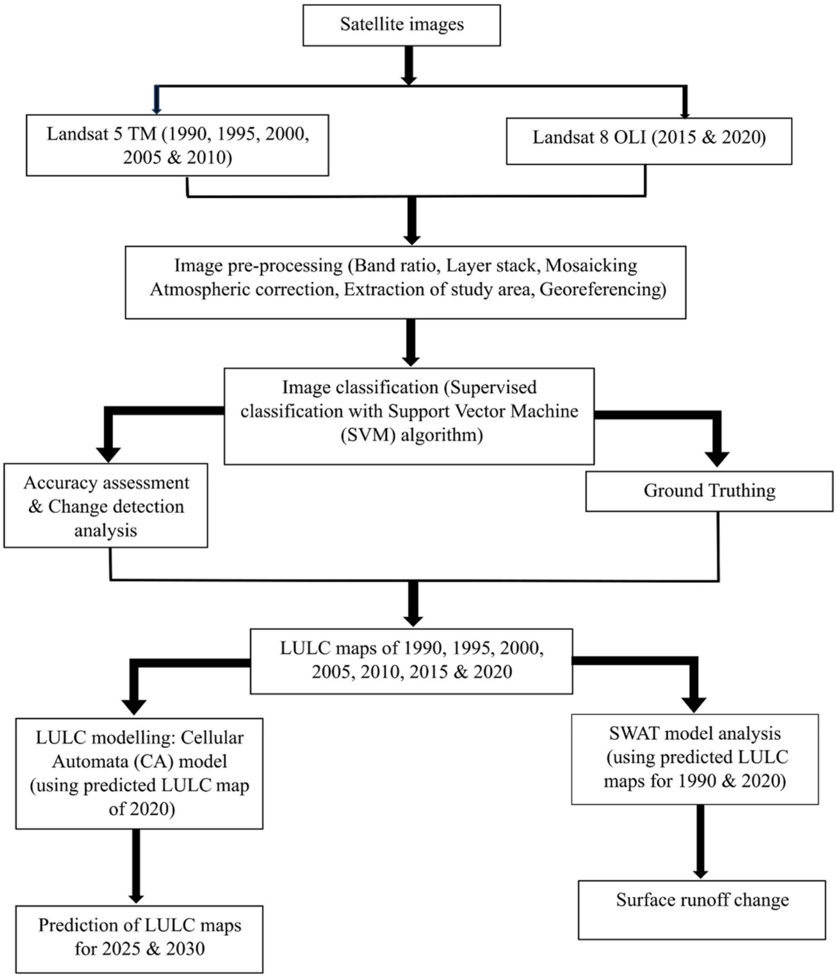

Fig. 2. Overview of the methodology of this study.

riod. Conversely, built-up acquired a UA ranging from 80 to 100% for all years. In general, all LULC classes attained a UA in the range of 80–100% for all years, except for natural vegetation in 1990, which attained a UA of 77.73%.

The LULC classes in this study achieved TD separability measures from 1.86 up to 2.00. Built-up areas attained relatively low separability measures particularly with bare land; while waterbody generally attained relatively high separability measures with five LULC classes.

4.2. LULC change detection over time

The spatial distribution of LULC in the Luvuvhu catchment from 1990 to 2020 is shown in Fig. 3. In general, bare land and natural vegetation were the most dominant land cover types for the study period. From 1990 to 2020, natural vegetation occupied 50%–80% of the catchment, while bare land occupied up to 45% of the catchment. On the other hand, waterbodies occupied $<1\%$ of the area, thus making it the smallest LULC in terms of area coverage. In general, waterbodies, plantation, and agricultural land, occupied less than 6% of the catchment for the entire study period. Natural vegetation suffered extensive loss of up to 1121.730 km^2 from 1990 to 2020. Part of natural vegetation was lost to built-up and agricultural land particularly in the Upper Luvuvhu catchment where agricultural activities are extensive. Furthermore, due to the population growth that has occurred over the study period, the catchment experienced urban expansion, hence the substantial increase in built-up. Built-up area revealed a continuous increase over the study period. The total area under this LULC class has been 29.9 km^2, 120.4 km^2, 314 km^2 in 1990, 2005 and 2020, respectively. The tremendous increase in this category can be attributed to the expansion of residential and commercial establishment. Bare land is the second most dominant LULC class in the Luvuvhu catchment. This class experienced an increase of up to 899.8 km^2 from 1990 to 2020. Bare land dominates the north-west part of the Lower Luvuvhu catchment and is rarely exploited by other LULC classes. The occurrence of bare land in the lower part of the catchment can be attributed to the unfavourable climatic conditions of the area. The lower area of the catchment is characterized by high annual temperature and receives low annual rainfall (Kundu et al., 2015) (see Fig. 4).

Table 4
Accuracy assessment of LULC classification in the study area.

1990				
Overall accuracy	94.3			
Kappa coefficient	0.93			
Individual accuracy	**Producer's accuracy**	**User's accuracy**	**Commission error**	**Omission error**
Waterbody	99.16	99.72	0.28	0.84
Plantation	99.86	99.59	0.41	0.14
Agricultural Land	97.93	98.71	1.29	2.07
Natural Vegetation	99.85	77.73	22.27	0.15
Bare Land	93.22	98.40	1.60	6.78
Built-up	70.03	100.00	0.00	29.97
1995				
Overall accuracy	93.48			
Kappa coefficient	0.91			
Waterbody	97.25	100.00	0.00	2.75
Plantation	96.32	86.50	13.50	3.68
Agricultural Land	70.53	100.00	0.00	29.47
Natural Vegetation	99.66	92.49	7.51	0.34
Bare Land	100.00	94.84	5.16	0.00
Built-up	70.26	100.00	0.00	29.74
2000				
Overall accuracy	95.76			
Kappa coefficient	0.95			
Waterbody	100.00	100.00	0.00	0.00
Plantation	97.48	100.00	0.00	2.52
Agricultural Land	98.33	93.41	6.59	1.67
Natural Vegetation	100.00	94.98	5.02	0.00
Bare Land	98.53	92.13	7.87	1.47
Built-up	70.01	100.00	0.00	29.99
2005				
Overall accuracy	96.61			
Kappa coefficient	0.96			
Waterbody	99.19	94.25	5.75	0.81
Plantation	92.59	99.81	0.19	7.41
Agricultural Land	99.81	91.20	8.80	0.19
Natural Vegetation	93.51	96.16	3.84	6.49
Bare Land	99.54	98.79	1.21	0.46
Built-up	86.52	97.07	2.93	13.48
2010				
Overall accuracy	94.10			
Kappa coefficient	0.9261			
Waterbody	100.00	100.00	0.00	0.00
Plantation	78.01	100.00	0.00	21.99
Agricultural Land	98.82	100.00	0.00	1.18
Natural Vegetation	100.00	83.89	16.11	0.00
Bare Land	98.99	97.04	2.96	1.01
Built-up	75.31	98.92	1.08	24.69
2015				
Overall accuracy	95.75			
Kappa coefficient	0.95			
Waterbody	100.00	99.55	0.45	0.00
Plantation	99.16	100.00	0.00	0.84
Agricultural Land	96.20	98.33	1.67	3.80
Natural Vegetation	98.33	87.65	12.35	3.62
Bare Land	91.83	97.95	2.05	8.17
Built-up	95.34	80.83	19.17	4.66
2020				
Overall accuracy	98.58			
Kappa coefficient	0.95			
Waterbody	100.00	100.00	0.00	0.00
Plantation	97.59	99.42	0.58	2.41
Agricultural Land	99.06	100.00	0.00	0.94
Natural Vegetation	99.34	97.51	2.49	0.66
Bare Land	98.52	98.13	1.87	1.48
Built-up	90.94	92.49	7.51	9.06

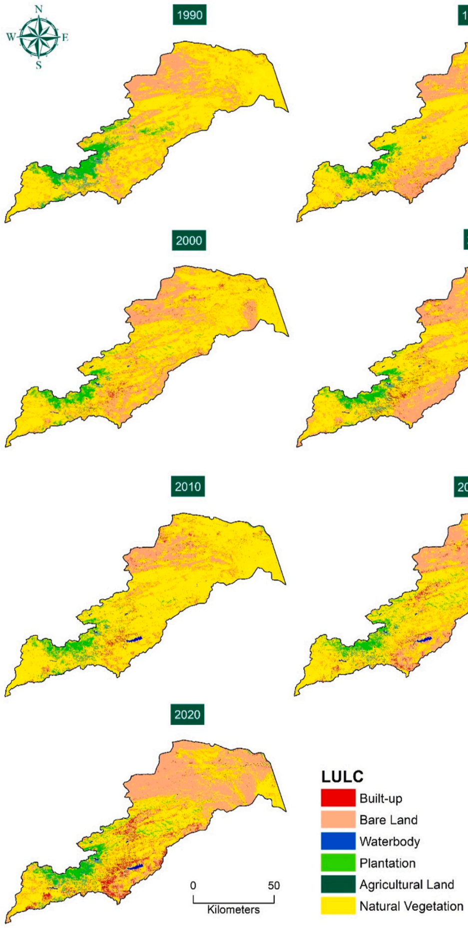

Fig. 3. LULC classification maps for the study period.

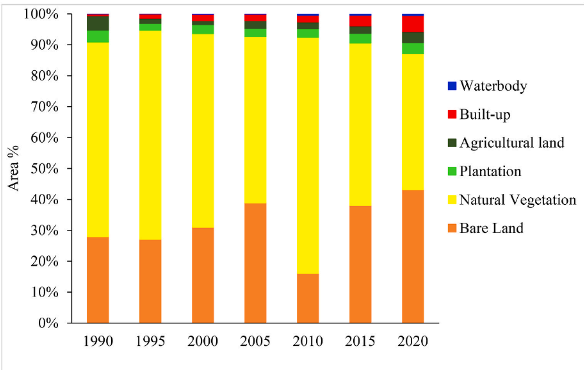

Fig. 4. Changes in the proportions of areas under different LULC types.

4.3. LULC spatial and temporal projections

The trends and projected area for the different LULC for 2020, 2025 and 2030 are shown in Fig. 5. From 2020 to 2025, built-up will increase by about 120 km^2, plantation by 17 km^2, agricultural land by 51 km^2 and bare land by 168 km^2. However, natural vegetation will lose up to 356 km^2 in 2025. Waterbody may lose close to 2 km^2 of area coverage from 2020 to 2025. Waterbody is most likely to change to natural vegetation than other LULC classes. The predicted LULC trends are expected to continue from 2025 to 2030, with natural vegetation being the LULC most susceptible to conversion to other LULC classes. As population growth persist, the volume of water in current waterbodies within the Luvuvhu catchment may decrease due to high water consumption. This corresponds with the study of Oberholster et al. (2008), which predicted that, by the year 2025, the quantity of water sources in Luvuvhu

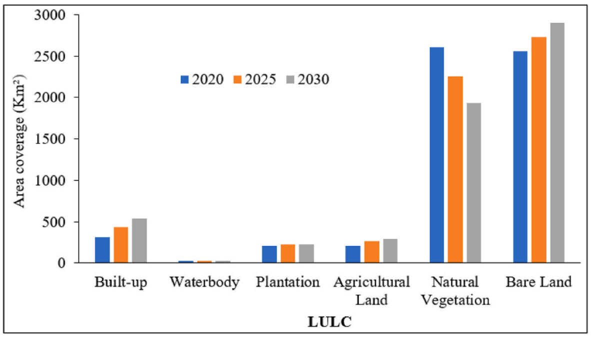

Fig. 5. Trends and predictions of LULC types from 2020 to 2030.

catchment will be reduced and this could lead to the water supply not meeting the demand. Therefore, waterbody will continue to decrease provided there are no dam constructions in the Luvuvhu catchment for the predicted years. While natural vegetation decreases by almost 316 km^2. Agricultural land is expected to continue to increase by 35 km^2, bare land by 176 km^2, built-up area by 104 km^2 and plantation by 1 km^2. The model validation results showed that overall accuracy and overall Kappa were 84.12 and 0.75, respectively.

The changes in predicted area coverage from 2020 to 2030 are shown in Table 5. From 2020 to 2025, bare land was projected to increase by 2.838%, followed by built-up areas, with 2.041%. On the other hand, natural vegetation will experience the largest loss by −6.012%, whereas waterbodies will experience the least decrease by −0.031%. From 2025 to 2030, The same trend was projected, where natural vegetation will continue to decrease by −5.325%, which is the largest decrease.

The projected spatial distribution of the different LULC types for 2025 and 20230 are shown in Fig. 6. The maps illustrate the predicted spatial distribution trends of the different LULC types from 2025 to 2030 across the study area.

4.4. Model performance evaluation

The calibration and validation statistics for LULC map for 1990 and 2020 are shown in Table 6. The model evaluation was based on statistical criteria, which include the Nash-Sutcliffe efficiency (NSE), the coefficient of determination (R^2), and percent bias (PBIAS). Model performance for the calibrated period using 1990 LULC map show satisfactory results with an R^2 value of 0.76, NSE of 0.68 and PBIAS of 0.9. On the other hand, the validation model performance was recorded with an R^2 value of 0.64, NSE of 0.54 and PBIAS of −31.8. The model performance results for the 2020 LULC map in the calibration period shows R^2 value of 0.75, NSE of 0.69 and PBIAS of −4.3 while validation results show R^2 value of 0.63, NSE of 0.53 and PBIAS of −33.0. These results show general overestimation of the model due to negative PBIAS. However, the NSE, R^2 and PBIAS results for the calibration periods appear to be better than those recorded for validation periods (see Table 7).

Table 5
LULC trends and projections from 2020 to 2030 in the catchment.

LULC	Area %					
	2020	2025	Δ	2025	2030	Δ
Built-up	5.299	7.339	2.041	7.339	9.088	1.748
Waterbody	0.504	0.473	−0.031	0.473	0.460	−0.013
Plantation	3.523	3.817	0.295	3.817	3.835	0.018
Agricultural Land	3.535	4.404	0.869	4.404	4.997	0.594
Natural Vegetation	44.008	37.996	−6.012	37.996	32.672	−5.325
Bare Land	43.132	45.970	2.838	45.970	48.948	2.978

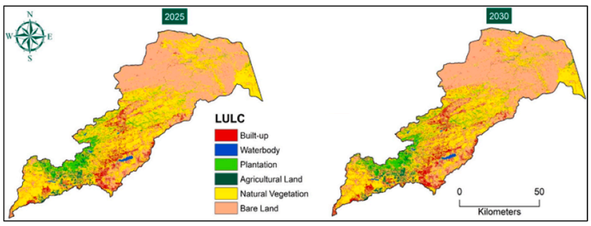

Fig. 6. Projected LULC trends for 2025 and 2030 in the Luvuvhu catchment.

Table 6
Model performance results for calibration and validation.

Model performance criteria		1990 LULC	2020 LULC
NSE	Calibration	0.68	0.69
	Validation	0.54	0.53
R^2	Calibration	0.76	0.75
	Validation	0.64	0.63
PBIAS	Calibration	0.9	−0.4
	Validation	−31.8	−33.0

Table 7
Effect LULC change on surface runoff.

LULC type	LULC Change from 1990 to 2020 (%)	Change in runoff (%)
Built-up	4.793	7.3%
Water body	0.416	
Plantation	−0.322	
Agricultural Land	1. 2	
Natural Vegetation	−18.933	
Bare Land	15.188	

4.5. The impacts LULC changes on surface runoff

A comparison of LULC maps for the years 1990, 1995, 2000, 2005, 2010 and 2020 indicates that the LULC classes in the Luvuvhu catchment were altered. Built-up area showed a significant increase of 4.8% in the period from 1990 to 2020. The greatest built-up increase occurred in the later years from 2015 to 2020. Agricultural land showed a fluctuation in the period from 1990 to 2020, however overall results show a decrease from 4.7% to 3.5%. Plantation and natural vegetation show a decrease of 0.3% and 18.9% from 1990 to 2020, respectively. Lastly, bare land in the Luvuvhu catchment increased by 15.2%. The simulation results from the two LULC periods showed changes in all hydrological components. The mean annual surface runoff increased from 169.14 mm to 181.49 mm between 1990 and 2020. On average, overall surface runoff increased by 7.3%. In contrast, evapotranspiration decreased from 279.7 mm to 275.08 mm.

5. Discussion

This study aimed to assess Land Use and Land Cover (LULC) alterations spanning the period from 1990 to 2020. Additionally, predictive modelling techniques were employed to forecast anticipated LULC changes for the years 2025 and 2030. Furthermore, the study endeavored to evaluate the consequential impact of these LULC alterations on run-off dynamics.

5.1. Spatial distribution of LULC from 1990 to 2020

The patterns of LULC variations in the catchment were estimated from Landsat images using SVM algorithm. The spatial distribution of LULC in the Luvuvhu catchment from 1990 to 2020 was evaluated. Over the past three decades, plantation and agricultural land were mostly found in the western part of Upper Luvuvhu catchment. The plantation category is dominated by Eucalyptus plantations which are the most preferred commercial timber plantations in the region since they can generate up to 10 times as much timber per hectare than native species (Bate et al., 1999; Kundu et al., 2015). Plantation was noted to reveal two change patterns during the study period. In 1990, plantation covered an area of 227.9 km^2 then declined by 96.080 km^2 in 1995, which can be attributed to timber harvesting and forest removal for commercial agriculture and built-up areas. An increasing trend of plantation can be noted from 2005 to 2020, with the catchment having second highest plantation coverage in 2020. Plantation such as Eucalyptus is a major contributor to the country's economy, thus the increasing trend from 152.9 km^2 in 2005 to 208.8 km^2 in 2020. Although the coverage of plantation flactuates due to production over the years, this LULC class shows an overall decrease from 227.9 km^2 in 1990 to 208.8 km^2 in 2020. Regardless of vast economic benefits, Eucalyptus plantations may pose many ecological problems such as reducing stream flow and dams levels (Hoogar et al., 2019). In this catchment, the Vondo dam is one of the most important dams for the supply of water to irrigation schemes and communities in the western parts of the Upper Luvuvhu catchment (Kundu et al., 2015).

Although, it is evident in the classification maps that a significant part of the agricultural (cultivated) land spatially falls closer to the plantation region, agricultural land has expanded towards the low lying areas of the catchment. Large scale commercial agricultural activities are mostly found near the Albasin Dam in the Levubu area, while the northern highlands and the riverbanks mostly consists of small scale and subsistence farming (Mukwada et al., 2021). The Luvuvhu catchment area is an underdevoloped and economically poor community. Therefore, subsistence farming has increased food security, and has played a major role in reducing unemployment in the Luvuvhu catchment. From 1995 to 2020, over a twofold increase of area coverage of agricultural land occurred. Despite numerous benefits from this land cover, agricultural land which depends on surface water bodies for irrigation during dry seasons, can further reduce available water. It has been reported that significant irrigation developments in the Upper Luvuvhu Catchment have resulted in a decrease in water for domestic and industrial supply (Muavhi and Mutoti, 2022).

Waterbody occupied about 5 km^2 of the total area in 1990, which dropped to 3 km^2 in 1995. The catchment experienced about threefold increase of waterbody area coverage up to 9 km^2 by 2000. The year 2000 marked one of the heavy rainfall periods in the catchment and severe socio-economic impacts triggered by this heavy rainfall (CRIDF, 2018). The overland flow of rainwater contributed to the increase in the overall area coverage of surface waterbodies. Post 2000, the region suffered several episodes of drought from 2002 to 2004 (Mazibuko et al., 2021). Therefore, in 2005 the area coverage of waterbody decreased to 7 km^2. The year 2005 also marked the completion of the Nandoni Dam, which makes up the Nandoni Dam sub-system, the largest and most recent development in the Luvuvhu Catchment. The main purpose of this dam is for regional water supply to Malamulele, Thohoyandou, Louis Trichardt, and surrounding areas as well as the revitalization of 11 km^2 subsistence irrigation schemes (DWA, 2012). From 2010 to 2020 the area coverage of waterbody gradually increased from 24 km^2 in 2010, 25 km^2 in 2015 to 29 km^2 in 2020. The 11 km^2 of Nandoni Dam contributed to the six-fold increase of waterbody in the catchment from 1990 (5 km^2) to 2020 (29 km^2). In general, bare land and natural vegetation were the most dominant land cover types for the study period.

From 1990 to 2020, natural vegetation occupied 50%–80% of the catchment, while bare land occupied up to 45% of the catchment. On the other hand, waterbodies occupied $<1\%$ of the area, thus making it the smallest LULC in terms of area coverage. In general, waterbodies, plantation, and agricultural land, occupied less than 6% of the catchment for the entire study period. Natural vegetation suffered extensive loss of up to 1121.730 km^2 from 1990 to 2020. Part of natural vegetation was lost to built-up and agricultural land particularly in the Upper Luvuvhu catchment where agricultural activities are extensive. Furthermore, due to the population growth that has occurred over the study period, the catchment experienced urban expansion, hence the substantial increase in built-up. Built-up area revealed a continuous increase over the study period. The total area under this LULC class has been 29.9 km^2, 120.4 km^2, 314 km^2 in 1990, 2005 and 2020, respectively. The tremendous increase in this category can be attributed to the expansion of residential and commercial establishment.

Bare land is the second most dominant LULC class in the Luvuvhu catchment. This class experienced an increase of up to 899.8 km^2 from 1990 to 2020. Bare land dominates the north-west part of the Lower Luvuvhu catchment and is rarely exploited by other LULC classes. The occurrence of bare land in the lower part of the catchment can be attributed to the unfavourable climatic conditions of the area. The lower area of the catchment is characterized by high annual temperature and receives low annual rainfall (Kundu et al., 2015). However, flash floods, which are common in the catchment may result in, sheet, rill, and gully erosion (CRIDF, 2018). Furthermore, the increase in bare land may be due to the removal of vegetation cover due to overgrazing, wood consumption and clay mining (State of Rivers Report, 2001). As stated previously, soil erosion reduces the land productivity and can cause sedimentation of catchments downstream, which has negative impacts on water quality and aquatic life (Kundu et al., 2015).

High overall accuracies were produced for the classified maps, ranging from 93% to 98% and Kappa coefficients above 0.9, which represents good classification (Aronoff, 1982; Altman, 1991; Muavhi, 2020). The confusion matrix reported a PA of $<80\%$ for built-up areas in 1990, 1995, 2000 and 2010. These were the years in which built-up areas achieved the lowest PA. Objects such as buildings and roads can be difficult to identify in low and medium spatial resolution satellite images (i.e., 30 m of Landsat) (Bouzekri et al., 2015; Janiola and Puno, 2018). In addition, although the separability measures of >1.85 are acceptable (Latty and Hoffer, 1980), built-up achieved low separability measures with most LULC classes, particularly in the earlier years of the study period. However, in the later years of the study period i.e., 2015 and 2020, built-up reached a PA of 90%. As settlements and other infrastructures associated with built-up become dense over time, sensors with medium spatial resolution such as Landsat can allow excellent classification. Waterbody, natural vegetation, and bare land attained PA beyond 90% for the entire study period. Conversely, built-up acquired a UA ranging from 80 to 100% for all years.

In the case of built-up in 1990, since 70.03% of validation pixels are classified correctly as demonstrated by the PA, UA parameter is the ratio of correctly classified pixels of built-up (70.03%) and the total number of validation pixels from all LULC classes classified as built-up. In addition, the UA parameter also assesses if the remaining 29.97% representing the OE of validation pixels of built-up is incorrectly classified as fitting to the remaining five LULC classes. Jensen (1986) describes UA as the precision or reliability of an algorithm in classifying LULC type in the ground. Therefore, the higher UA implies that few to no pixels are misclassified as other LULC classes in the ground. Meanwhile, Muavhi (2020) considers UA as a parameter of estimating the level of confidence that can be attributed to pixels classified as belonging to a land cover type in an image. In general, all LULC classes attained a UA in the range of 80–100% for all years, except for natural vegetation in 1990, which attained a UA of 77.73%. Therefore, a confidence level beyond 80% can be attributed to all classified pixels in the LULC classification images. Consequently, the estimated main accuracy measures (overall accuracy and Kappa coefficient) and accuracies per class (PA, UA, CE, and OE) provide a major platform for the subsequent analysis of LULC spatial distribution and changes.

5.2. The impacts LULC changes on surface runoff

Literature suggests that the amount of change in catchment water yield is indirectly proportional to the percentage of forest cover of a catchment. Thus, an increase in vegetation cover results to a decrease in surface flow, while the removal of vegetation cover leads to an increase in surface flow (Affessa et al., 2022). The reduction of evapotranspiration influences the increase of runoff (Mishra et al., 2014). Evapotranspiration is higher in natural forests than on land cover with sparse vegetation (Owuor et al., 2016). Therefore, the removal of vegetation cover reduces evapotranspiration and increases the rate of surface runoff. Water yield showed little to no change from 557.2 mm to 557.06 mm. Astuti et al. (2019) states that change in water yield is mostly due to an increase in surface runoff, however in this study only a 7% increase was observed, thus the negligible change in water yield. Increase in surface runoff also leads to reduced infiltration and a decrease in ground water recharge (Mishra et al., 2014). However, the impact of LULC change on groundwater is not discussed in this study. The variation of the hydrological components over the study period supports the impact of LULC changes. The resulting increase in catchment discharge observed in this study was influenced by the LULC changes that occurred in the catchment. The subsequent 18.9% decrease in natural vegetation and the 15.2% increase in bare land caused the change in hydrological components. Serpa et al. (2015) stated that, deforested lands have high surface runoff and low groundwater recharge than forest areas. Furthermore, agricultural land and bare land require less soil moisture than forest cover or plantation, and rainfall satisfies the soil moisture deficit in these land cover classes more rapidly than in plantation, thus leading to high runoff generation (Deng et al., 2015). Therefore, the LULC changes observed in this study align with the literature, that the reduction of natural vegetation and plantation decreases infiltration thus leading to increased surface runoff (Chilagane et al., 2021).

5.3. Effect of LULC change on SWAT model parameter posterior distribution

The impact of LULC change on the SWAT model's parameter posterior distribution holds significant implications for hydrological modelling, a notion articulated by Abbaspour et al. (2007) and reinforced by Faramarzi et al. (2010). As landscapes undergo dynamic transformations driven by urbanization, deforestation, and agricultural expansion, there arises a critical need for SWAT model parameters to adapt, ensuring an accurate representation of evolving hydrological processes (Neitsch et al., 2005; Moriasi et al., 2007a,b). These alterations, affecting land cover types, soil properties, and vegetation, mandate a comprehensive reassessment of the model's parameter posterior distribution, a point underscored (Gassman et al., 2007; Gosain et al., 2013).

The intricate interplay between LULC changes and SWAT model parameters becomes particularly evident in regions experiencing rapid land use transformations, as exemplified by the Luvuvhu Catchment. In these areas, the precision of SWAT model simulations is contingent on accurate representations of current landscape dynamics within its parameters (J. G Arnold et al., 2012; Gassman et al., 2007). A holistic understanding of the complex relationships between LULC changes and SWAT model parameter posterior distribution is essential for refining hydrological simulations and ensuring robust predictive capabilities under changing environmental conditions (Huang et al., 2018; Shafiei et al., 2020). However, to advance our knowledge in this field, it is imperative for future studies to delve deeper into the effect of LULC change on SWAT model parameter posterior distribution in catchments akin to the Luvuvhu. The observed trends in 2025 are anticipated to persist until 2030, signifying the enduring nature of LULC-induced changes. The outcomes of the Luvuvhu catchment study indicated a 7.3% increase in overall surface runoff between 1990 and 2020, with significant contributions from LULC changes in bare land and natural vegetation (Magidi et al., 2021; Xu et al., 2015). These alterations, representing a 15.2% increase and an 18.9% decrease, respectively, substantially influenced the catchment's runoff response. The expectation of ongoing LULC alterations suggests a sustained increase in surface runoff, presenting challenges such as flooding and erosion. Consequently, the prioritization of effective catchment management strategies is crucial to mitigate the impacts of LULC changes, as emphasized by the findings of this study, offering valuable baseline information on the effects of LULC changes on surface runoff in the Luvuvhu catchment in Limpopo, South Africa. Further studies in analogous catchments will deepen our understanding and guide adaptive management strategies (Zuo et al., 2019; Waramboi et al., 2023).

6. Conclusion

The study aimed to comprehensively assess the impact of LULC changes on surface runoff within the Luvuvhu catchment from 1990 to 2020, utilizing remotely sensed data and predictive modelling techniques. Our analyses unveiled significant alterations in the Luvuvhu catchment, notably marked by a 15.2% increase in bare land and an alarming 18.9% reduction in natural vegetation cover. These transformations were linked to a 7.3% surge in mean annual surface runoff over the evaluated period, signifying a potential shift in the catchment's hydrological dynamics. The observed decline in natural vegetation alongside the proliferation of bare land emerged as pivotal contributors to the amplified surface runoff. These changes may instigate various environmental challenges, including heightened flood risks, erosion of riverbanks, and increased peak flow rates, posing significant threats to the catchment's sustainability. Implications drawn from our findings underscore the urgency for proactive management strategies. To curtail the degradation and subsequent impacts on surface runoff within the catchment, it's imperative to prioritize sustainable land use practices. This necessitates robust regulatory frameworks and adaptive land management policies to control and guide LULC alterations. Furthermore, fostering ecosystem restoration initiatives and promoting afforestation programs could aid in mitigating the adverse effects of reduced vegetation cover. Encouraging sustainable agricultural practices and advocating for responsible urban development are crucial steps toward maintaining the balance between land use changes and hydrological stability. In essence, this study emphasizes the critical need for coordinated efforts among stakeholders, policymakers, and land managers to implement sustainable land management practices. By adopting a proactive and holistic approach, we can mitigate the degradation of the catchment and promote long-term sustainability of water resources within the Luvuvhu catchment.

Ethical issues

No ethical issues to declare.

CRediT authorship contribution statement

Mpho Oscar Mabuda: Writing – original draft, Validation, Methodology, Investigation, Formal analysis, Data curation, Conceptualization. **Cletah Shoko:** Writing – review & editing, Writing – original draft, Supervision, Methodology, Funding acquisition, Formal analysis, Data curation, Conceptualization. **Timothy Dube:** Writing – original draft, Resources, Methodology, Formal analysis, Conceptualization. **Dominic Mazvimavi:** Data curation, Conceptualization.

Declaration of competing interest

The authors declare no conflicts of interest related to this research work.

Data availability

Data will be made available on request.

References

Abbas, T., Nabi, G., Boota, M.W., Hussain, F., Azam, M.I., Jin, H., Faisal, M., 2016. Uncertainty analysis of runoff and sedimentation in a forested watershed using sequential uncertainty fitting method. Sciences in Cold and Arid Regions 8 (4), 297–310.

Abbaspour, K.C., Yang, J., Maximov, I., Srinivasan, R., Zehnder, A.J., 2007. Modelling hydrology and water quality in the pre-alpine/alpine Thur watershed using SWAT. J. Hydrol. 333 (2–4), 413–430.

Abd El-Kawy, O.R., Rød, J.K., Ismail, H.A., Suliman, A.S., 2011. Land use and land cover change detection in the western Nile delta of Egypt using remote sensing data. Appl. Geogr. 31 (2), 483–494.

Abijith, D., Saravanan, S., 2022. Assessment of land use and land cover change detection and prediction using remote sensing and CA Markov in the northern coastal districts of Tamil Nadu, India. Environ. Sci. Pollut. Control Ser. 29 (57), 86055–86067.

Affessa, G.M., Belew, A.Z., Tenagashaw, D.Y., Tamirat, D.M., 2022. Land use/cover change impacts on hydrology using SWAT model on Borkena watershed, Ethiopia. Water Conservation Science and Engineering 7 (1), 55–63.

Alawamy, J.S., Balasundram, S.K., Mohd. Hanif, A.H., Boon Sung, C.T., 2020. Detecting and analyzing land Use and land cover changes in the region of Al-Jabal Al-Akhdar, Libya Using time-series Landsat data from 1985 to 2017. Sustainability 12 (11), 4490.

Altman, D.G., 1991. Practical Statistics for Medical Research. Chapman and Hall, London.

Anand, J., Gosain, A., Khosa, R., 2018. Prediction of land use changes based on Land Change Modeler and attribution of changes in the water balance of Ganga basin to land use change using the SWAT model. Sci. Total Environ. 644, 503–519.

Arnold, J.G., Moriasi, D.N., Gassman, P.W., Abbaspour, K.C., White, M.J., Srinivasan, R., Harmel, R.D., 2012. SWAT: model use, calibration, and validation. Transactions of the ASABE 55 (4), 1491–1508.

Arnold, J.G., Moriasi, D.N., Gassman, P.W., Abbaspour, K.C., White, M.J., Srinivasan, R., Santhi, C., Harmel, R.D., van Griensven, A., Van Liew, M.W., Kannan, N., Jha, M.K., 2012. SWAT: model use, calibration and validation. American Society of Agricultural and Biological Engineers 55, 1491–1508.

Aronoff, S., 1982. The map accuracy report-A user's view. Photogramm. Eng. Rem. Sens. 48 (8), 1309–1312.

Astuti, I.S., Sahoo, K., Milewski, A., Mishra, D.R., 2019. Impact of land use land cover (LULC) change on surface runoff in an increasingly urbanized tropical watershed. Water Resour. Manag. 33, 4087–4103.

Bagaria, P., Nandy, S., Mitra, D., Sivakumar, K., 2021. Monitoring and predicting regional land use and land cover changes in an estuarine landscape of India. Environ. Monit. Assess. 193, 1–27.

Ban, Y., Yousif, O., 2016. Change detection techniques: a review. In: Ban, Y. (Ed.), Multitemporal Remote Sensing. Remote Sensing and Digital Image Processing, vol. 20. Springer, Cham.

Bate, R.R., Tren, R., Mooney, L., 1999. An Econometric and Institutional Economic Analysis of Water Use in the Crocodile River Catchment, Mpumalanga Province, South Africa, WRC Report No. 885/1/99, Pretoria, South Africa.

Bouzekri, S., Lasbet, A.A., Lachehab, A., 2015. A new spectral index for extraction of built-up area using Landsat-8 data. Journal of the Indian Society of Remote Sensing 43, 867–873.

Chilagane, N.A., Kashaigili, J.J., Mutayoba, E., Lyimo, P., Munishi, P., Tam, C., Burgess, N., 2021. Impact of land use and land cover changes on surface runoff and sediment yield in the Little Ruaha River Catchment. Open J. Mod. Hydrol. 11 (3), 54–74.

CRIDF (Climate Resilient Infrastructure Development Facility), 2018. Investing £24,000 in Flood Forecasting Systems in the Limpopo River Basin Saves £140,000 Per Annum in Flood Damage.

Deng, X., Shi, Q., Zhang, Q., Shi, C., Yin, F., 2015. Impacts of land use and land cover changes on surface energy and water balance in the Heihe River Basin of China, 2000–2010. Phys. Chem. Earth, Parts A/B/C 79–82, 2–10.

Devia, G., Ganasri, B., Dwarakish, G., 2015. A review on hydrological models. Aquatic Procedia 4, 1001–1007.

DWA – Department of Water Affairs, 2012. Minister Establishes Nine (9) Catchment Management Agencies, March 30th 2012. DWA, Pretoria.

Faramarzi, M., Abbaspour, K.C., Vaghefi, S., Srinivasan, R., 2010. A new approach to uncertainty analysis of SWAT model predictions. J. Hydrol. 381 (1–2), 203–213.

Gassman, P.W., Reyes, M.R., Green, C.H., Arnold, J.G., 2007. The Soil and Water Assessment Tool: historical development, applications, and future research directions. Transactions of the ASABE 50 (4), 1211–1250.

Gessesse, B., Bewket, W., Bräuning, A., 2014. Model-based characterization and monitoring of runoff and soil erosion in response to land use/land cover changes in the Modjo watershed, Ethiopia. Land Degrad. Dev. 26 (7), 711–724.

Getahun, Yitea, Haj, Van., 2015. Assessing the impacts of land use-cover change on hydrology of Melka Kuntrie Subbasin in Ethiopia, using a conceptual hydrological model. Journal of Wastewater Treatment & Analysis 6. https://doi.org/10.4172/2157-7587.1000210.

Ghosh, P., Mukhopadhyay, A., Chanda, A., Mondal, P., Akhand, A., Mukherjee, S., Nayak, S.K., Ghosh, S., Mitra, D., Ghosh, T., Hazra, S., 2017. Application of Cellular automata and Markov-chain model in geospatial environmental modeling- A review. Remote Sens. Appl.: Society and Environment 5, 64–77.

Gosain, A.K., Rao, S., Basuray, D., 2013. Integrated modeling for water resources assessment and management. J. Hydrol. Eng. 18 (4), 377–386.

Griscom, H.R., Miller, S.N., Gyedu-Ababio, T., Sivanpillai, R., 2009. Mapping land cover change of the Luvuvhu catchment, South Africa for environmental modelling. Geojournal 75 (2), 163–173.

Guo, Y., Fang, G., Xu, Y.-P., Tian, X., Xie, J., 2020. Identifying how future climate and land use/cover changes impact streamflow in Xinanjiang Basin, East China. Sci. Total Environ. 710, 136275.

Hakim, A.M.Y., Baja, S., Rampisela, D.A., Arif, S., 2019. Spatial dynamic prediction of land use land cover change (case study: Tamalanrea sub-district, Makassar city). In: IOP Conference Series: Earth and Environmental Science, vol. 280. Institute of Physics Publishing, 012023.

Hoogar, R., Malakannavar, S., Sujatha, H.T., 2019. Impact of eucalyptus plantations on ground water and soil ecosystem in dry regions. J. Pharmacogn. Phytochem. 8 (4), 2929–2933.

Hope, R., Jewitt, G., Gowing, J., 2004. Linking the hydrological cycle and rural livelihoods: a case study in the Luvuvhu catchment, South Africa. Phys. Chem. Earth, Parts A/B/C 29 (15–18), 1209–1217.

Huang, S., Xu, Y., Sun, Z., Wang, W., Lei, X., 2018. Impact of land use change on hydrological processes in a typical watershed of the Loess Plateau. Sustainability 10 (12), 4577.

Janiola, M.D.C., Puno, G.R., 2018. Land use and land cover (LULC) change detection using multi-temporal Landsat imagery: a case study in Allah Valley Landscape in Southern, Philippines. J. Biodivers. Environ. Sci. (JBES) 12 (2), 98–108.

Jensen, J.R., 1986. Introductory Digital Image Processing. Prentice-Hall, New Jersey, Englewood Cliffs.

Jewitt, G.P.W., Garratt, J.A., Calder, I.R., Fuller, L., 2004. Water resources planning and modelling tools for the assessment of land use change in the Luvuvhu Catchment, South Africa. Phys. Chem. Earth, Parts A/B/C 29 (15–18), 1233–1241.

Jogun, T., Lukić, A., Gašparović, M., 2019. Simulation model of land cover changes in a post-socialist peripheral rural area: Požega-Slavonia County, Croatia. Hrvat. Geogr. Glas. 81 (1), 31–59.

Kundu, P., Mathivha, T., Nkuna, T., 2015. The Use of GIS and Remote Sensing Techniques to Evaluate the Impact of Land Use and Land Cover Change on the Hydrology of Luvuvhu River Catchment in Limpopo Province. WRC Report No. 2246/1/15, Pretoria, South Africa.

Lambin, E., Turner, B., Geist, H., Agbola, S., Angelsen, A., Bruce, J., Coomes, O., Dirzo, R., Fischer, G., Folke, C., George, P., Homewood, K., Imbernon, J., Leemans, R., Li, X., Moran, E., Mortimore, M., Ramakrishnan, P., Richards, J., Skånes, H., Steffen, W., Stone, G., Svedin, U., Veldkamp, T., Vogel, C., Xu, J., 2001. The causes of land-use and land-cover change moving beyond the myths. Global Environ. Change 11 (4), 261–269.

Latty, R.S., Hoffer, R.M., 1980. Waveband evaluation of proposed Thematic Mapper in forest cover classification. In: Proc. Of the Fall Technical Meeting. ACSM-ASP, Niagara Falls, New York, pp. 1–12.

Lin, B., Chen, X., Yao, H., Chen, Y., Liu, M., Gao, L., James, A., 2015. Analyses of landuse change impacts on catchment runoff using different time indicators based on SWAT model. Ecol. Indicat. 58, 55–63.

Lothar, H., Dieter, F., Puzicha, J., Buhmann, J.M., 1999. Support vector machines for land usage classification in LANDSAT TM imagery. Proc. of IGARSS 1, 348–350.

Magidi, J.M., Tadross, M., Gwate, O., 2021. Hydrological response to land use and land cover changes in a semi-arid catchment, Luvuvhu River, South Africa. Geocarto Int. 1–21.

Manoj, J., Subramonia, R.S., Srinivasan, K.S., Pathak, S., Sharma, J.R., 2013. Class separability analysis and classifier comparison using Quad-polarization Radar imagery. Journal of Indian Society of Remote Sensing 41 (1), 177–182.

Mathivha, F., Kundu, P., Singo, L., 2016. The Impacts of Land Cover Change on Stream Discharges in Luvuvhu River Catchment, Vhembe District, Limpopo Province, South Africa. *Urban Water III*.

Maviza, A., Ahmed, F., 2020. Analysis of past and future multi-temporal land use and land cover changes in the semi-arid Upper-Mzingwane sub-catchment in the Matabeleland south province of Zimbabwe. Int. J. Rem. Sens. 41 (14), 5206–5227.

Mazibuko, S.M., Mukwada, G., Moeletsi, M.E., 2021. Assessing the frequency of drought/flood severity in the Luvuvhu River catchment, Limpopo Province, South Africa. WaterSA 47 (2 April).

Mishra, N., Khare, D., Gupta, K.K., Shukla, R., 2014. Impact of land use change on groundwater—a review. Advances in Water Resource and Protection 2 (28), 28–41.

MOLUSCE, 2018. MOLUSCE Modules for Land Use Change Evaluation-Quick Help. https://github.com/nextgis/molusce/blob/master/doc/en/QuickHelp.pdf (Accessed 28 September 2021).

Moriasi, D.N., Arnold, J.G., Van Liew, M.W., Bingner, R.L., Harmel, R.D., Veith, T.L., 2007a. Model evaluation guidelines for systematic quantification of accuracy in watershed simulations. Transactions of the ASABE 50 (3), 885–900.

Moriasi, D.N., Arnold, J.G., Van Liew, M.W., Bingner, R.L., Harmel, R.D., Veith, T.L., 2007b. Model evaluation guidelines for systematic quantification of accuracy in watershed simulations. Transactions of the ASABE 50 (3), 885–900.

Muavhi, N., 2020. Evaluation of effectiveness of supervised classification algorithms in land cover classification using ASTER images-A case study from the Mankweng (Turfloop) Area and its environs, Limpopo Province, South Africa. S. Afr. J. Geol. 9 (1), 61–74.

Muavhi, N., Mutoti, M.I., 2022. Using Geospatial Techniques and Analytic Hierarchy Process to Map Groundwater Potential Zones. Groundwater [Preprint].

Mukwada, G., Mazibuko, S.M., Moeletsi, M., Robinson, G.M., 2021. Can famine be averted? A spatiotemporal assessment of the impact of climate change on food security in the Luvuvhu River Catchment of South Africa. Land 10 (5), 527.

Neitsch, S.L., Arnold, J.G., Kiniry, J.R., Williams, J.R., King, K.W., 2005. Soil and Water Assessment Tool (SWAT) Theoretical Documentation. Texas Water Resources Institute.

Ntanganedzeni, B., Nobert, J., 2020. Flood risk assessment in Luvuvhu River, Limpopo province, South Africa. Physics and Chemistry of the Earth. Parts A/B/C, 102959.

Oberholster, P.J., Botha, A.M., Cloete, T.E., 2008. Biological and chemical evaluation of sewage water pollution in the Rietvlei nature reserve wetland area, South Africa. Environ. Pollut. 156, 184–192.

Odiyo, J., Phangisa, J., Makungo, R., 2012. Rainfall–runoff modelling for estimating Latonyanda river flow contributions to Luvuvhu River downstream of Albasini dam. Phys. Chem. Earth, Parts A/B/C 50–52, 5–13.

Owuor, S., Butterbach-Bahl, K., Guzha, A., Rufino, M., Pelster, D., Díaz-Pinés, E., Breuer, L., 2016. Groundwater recharge rates and surface runoff response to land use and land cover changes in semi-arid environments. Ecological Processes 5 (1).

Ozdemir, H., Elbaşı, E., 2014. Benchmarking land use change impacts on direct runoff in ungauged urban watersheds. Phys. Chem. Earth, Parts A/B/C 79–82, 100–107.

Peng, T., Wang, S.-., 2012. Effects of land use, land cover and rainfall regimes on the surface runoff and soil loss on karst slopes in southwest China. Catena 90, 53–62.

Powell, R.L., Matzke, N., Souza, C.D., Clark, M., Numata, I., Hess, L.L., Roberts, D.A., 2004. Sources of error in accuracy assessment of Thematic land-cover maps in the Brazilian Amazon. Rem. Sens. Environ. 90 (2), 221–234.

Rahman, M.T.U., Tabassum, F., Rasheduzzaman, M., Saba, H., Sarkar, L., Ferdous, J., et al., 2017. Temporal dynamics of land use/land cover change and its prediction using CA-ANN model for southwestern coastal Bangladesh. Environ. Monit. Assess. 189, 1–18.

Richards, J.A., Jia, X., 2005. Remote Sensing Digital Image Analysis, fourth ed. Springer-Verlag, Berlin.

Santé, I., García, A.M., Miranda, D., Crecente, R., 2010. Cellular automata models for the simulation of real-world urban processes: a review and analysis. Landsc. Urban Plann. 96 (2), 108–122.

Serpa, D., Nunes, J., Santos, J., Sampaio, E., Jacinto, R., Veiga, S., Lima, J., Moreira, M., Corte-Real, J., Keizer, J., Abrantes, N., 2015. Impacts of climate and land use changes on the hydrological and erosion processes of two contrasting Mediterranean catchments. Sci. Total Environ. 538, 64–77.

Shafiei, M., Borhan, M.S., Fohrer, N., 2020. Evaluation of the SWAT model for land use and climate change impact assessment on streamflow in the Pahang River basin, Malaysia. Journal of Hydro-environment Research 28, 116–131.

Sidle, R., 2021. Strategies for smarter catchment hydrology models: incorporating scaling and better process representation. Geoscience Letters 8 (1).

Singh, V.G., Singh, S.K., Kumar, N., Singh, R.P., 2022. Simulation of land use/land cover change at a basin scale using satellite data and Markov chain model. Geocarto Int. 37 (26), 11339–11364.

State of Rivers Report, 2001. Letaba and Luvuvhu River Systems. WRC Report No: TT 165/01 Water Research Commission Pretoria ISBN No: 1 86845 82s.

Sterling, S., Ducharne, A., Polcher, J., 2012. The impact of global land-cover changes on the terrestrial water cycle. Nat. Clim. Change 3 (4), 385–390.

Thanekar, G.S., Krishna, R.V., 2021. Land Use Land Cover Prediction Analysis.

Thapa, P., 2021. The relationship between land use and climate change: a case study of Nepal. The Nature, Causes, Effects and Mitigation of Climate Change on the Environment.

Thavhana, M., Savage, M., Moeletsi, M., 2018. SWAT model uncertainty analysis, calibration and validation for runoff simulation in the Luvuvhu River catchment, South Africa. Phys. Chem. Earth, Parts A/B/C 105, 115–124.

Turner, M.G., Pearson, S.M., Bolstad, P., Wear, D.N., 2003. Effects of land-cover change on spatial pattern of forest communities in the southern Appalachian Mountains (USA). Landsc. Ecol. 18, 449–464.

Waramboi, J.G., Sharma, S., James, R., 2023. Impact of land-use and climate change on water resources in the Markham River catchment, Papua New Guinea. J. Hydrol.: Reg. Stud. 45, 102042.

Warburton, M.L., Schulze, R.E., Jewitt, G.P.W., 2012. Hydrological impacts of land use change in three diverse South African catchments. J. Hydrol. 414–415, 118–135.

Xu, C., Gong, L., Jiang, T., 2015. The effects of land use changes on soil erosion distribution in a karst watershed, Southwest China. Catena 127, 234–244.

Yadav, Y., 2019. Dynamics of land use land cover change and mapping of tree outside forest (TOF) in Terai, Nepal. International Journal of Environmental Sciences & Natural Resources 19 (1).

Yatoo, S.A., Sahu, P., Kalubarme, M.H., Kansara, B.B., 2020. Monitoring Land Use Changes and its Future Prospects Using Cellular Automata Simulation and Artificial Neural Network for Ahmedabad City, vol. 23. GeoJournal, India.

Zhang, P., Liu, R., Bao, Y., Wang, J., Yu, W., Shen, Z., 2014. Uncertainty of SWAT model at different DEM resolutions in a large mountainous watershed. Water Res. 53, 132–144.

Zuo, D., Xu, Z., Wang, W., Gao, W., 2019. Impacts of land use change on watershed hydrology and sediment transport: a case study of the Weihe River Basin, China. Sci. Total Environ. 654, 593–603.